Journal of Applied Polymer Science

Synthesis of poly(butyl acrylate-co-methyl methacrylate)/montmorillonite waterborne nanocomposite via semibatch emulsion polymerization

Alican Vatansever,[1] Tulay Y. Inan,[2] Hacer Dogan,[1] Ahmet Sirkecioglu[3]
[1]TÜBİTAK Marmara Research Center, Chemistry Institute, 41470 Gebze-Kocaeli, Turkey
[2]Saudi Aramco, PO BOX 5074, Dhahran 31311, Saudi Arabia
[3]Istanbul Technical University, Department of Chemistry and Metallurgy, Ayazaga, 34469 Istanbul, Turkey
Correspondence to: A. Vatansever (E-mail: alican.vatansever@tubitak.gov.tr) and T. Y. Inan (E-mail: tulayinan2012@gmail.com)

ABSTRACT: Poly(butyl acrylate-co-methyl methacrylate)-montmorillonite (MMT) waterborne nanocomposites were successfully synthesized by semibatch emulsion polymerization. The syntheses of the nanocomposites were performed in presence of sodium montmorillonite (Na-MMT) and organically modified montmorillonite (O-MMT). O-MMT was used directly after the modification of Na-MMT with dimethyl dioctadecyl ammonium chloride. Both Na-MMT and O-MMT were sonified to obtain nanocomposites with 47 wt % solids and 3 wt % Na-MMT or O-MMT content. Average particle sizes of Na-MMT nanocomposites were measured as 110–150 nm while O-MMT nanocomposites were measured as 200–350 nm. Both Na-MMT and O-MMT increased thermal, mechanical, and barrier properties (water vapor and oxygen permeability) of the pristine copolymer explicitly. X-ray diffraction and transmission electron microscope studies show that exfoliated morphology was obtained. The gloss values of O-MMT nanocomposites were found to be higher than that of the pristine copolymer. © 2015 Wiley Periodicals, Inc. J. Appl. Polym. Sci. **2015**, *132*, 42373.

KEYWORDS: clay; emulsion polymerization; mechanical properties; properties and characterization; thermal properties

Received 8 December 2014; accepted 16 April 2015
DOI: 10.1002/app.42373

INTRODUCTION

Many studies have been devoted to nano-reinforcement addition into polymers for improving features of polymers. Nano-reinforced polymer composite studies have mainly been focused on clays because toward the end of the twentieth century, the study on nylon-clay hybrids[1] has attracted a great deal of interest for polymer clay nanocomposites. Many researchers have shown that polymer clay nanocomposites (PCN) exhibit enhanced mechanical, thermal, electrical properties, and reduced gas permeability.[2–5]

Natural sodium montmorillonite (Na-MMT) is the most used smectite clay for PCN synthesis. The thickness and width of Na-MMT crystals are 1 and 200–600 nm, respectively. A PCN can be obtained by dispersing Na-MMT in a polymer matrix. PCNs are mainly synthesized by four processes; exfoliation-adsorption, template synthesis, melt intercalation, and in situ intercalative polymerization.[6] In order to synthesize waterborne PCNs, in situ intercalative polymerization is considered to be the most suitable method.[7–10] For a waterborne PCN with improved properties, Na-MMT should sufficiently disperse in the polymer matrix. Na-MMT is fully hydrated in water. Therefore, in-situ emulsion polymerization is commonly preferred for waterborne PCN synthesis.[11–19]

Since most of the monomers/polymers are hydrophobic, hydrophilic feature of Na-MMT can be altered to form organo-modified montmorillonite (O-MMT) by exchange of Na^+ with organic cations as quaternary ammonium cations. Those exchanged organic cations can increase interlayer spacing of Na-MMT, leading to enhanced polymer intercalation or even form highly exfoliated nanocomposites.

Lee and co-workers studied in situ emulsion polymerization in the presence of Na-MMT by using several monomers including methyl methacrylate (MMA), styrene, acrylo-nitrile styrene, and acrylo-nitrile butadiene styrene (ABS).[11–15] Later, some researchers used 2-Acrylamido-2-methylpropane sulfonic acid (AMPS) as surfactant for better interaction between Na-MMT and polymer.[16–19] Furthermore, there have been many studies focusing on O-MMT-polymer nanocomposites. Noh and Lee worked on O-MMT-PMMA hybrid through solution polymerization by dispersing dimethyl dihydrogenated tallow-MMT in cyclohexanone with addition of AIBN (2,2′-Azobis(2-methylpropionitrile)).[12] However, the PCN was not waterborne and

moreover, O-MMT did not exfoliate in the polymer. Yeh *et al.* used in-situ emulsion polymerization and tried to synthesize O-MMT nanocomposite by adding O-MMT directly in water but monomer/polymer could not be incorporated into O-MMT platelets since the stacks of highly hydrophobic clay did not disperse in water.[20] In some cases, O-MMT was dispersed in monomers such as styrene, MMT, and butyl acrylate (BA).[21–24] This procedure is conventional emulsion polymerization and also this type of polymerization could not provide highly exfoliated clay in polymer matrix.

Due to the exfoliation problem of O-MMT in conventional emulsion polymerization, some scientists used a technique similar to conventional polymerization called miniemulsion polymerization, where two immiscible liquid phases (mostly water and organic liquids) are sheared and at least one surfactant and one co-surfactant are used. The difference between conventional and miniemulsion polymerization lies in the nucleation mechanism. Particle formation is a mixture of micellar and homogenous nucleation in conventional polymerization while particles are formed by droplet in miniemulsion. Droplet is accomplished by using an appropriate surfactant and a highly hydrophobic co-surfactant with high shear mixing.[25–33] Miniemulsion studies in open literature generally used MMA, butyl acrylate (BA), styrene monomers, styrene–BA, and MMA–BA co-monomers in a batch process for obtaining PCNs. Solids content of the final PCNs was mostly below 25 wt %. However, commercial applications generally require at least 45 wt % solids content.[34]

Gabriela Diaconu and co-workers reported high solids content waterborne poly(BA-MMA)/MMT nanocomposites in semibatch process. In their study, emulsion polymerization system was used for Na-MMT–polymer nanocomposites and maximum clay content was 3 wt % of monomers while the resultant solids contents varied between 30 and 45 wt %. In their O-MMT–polymer nanocomposite study, miniemulsion polymerization system was performed through semibatch process. O-MMT content of the final nanocomposite was maximum 1.8 wt % of monomers and achieved solids content was 45 wt %.[34–36] According to the miniemulsion studies, miniemulsion is seemed to be the most suitable method for synthesizing waterborne O-MMT–polymer nanocomposites. However, at least one extra surfactant is needed in miniemulsion polymerization, which impact economic aspects and may show undesirable presence in the final product.[37] Furthermore, constant reaction rate cannot be observed and polymerization period is generally quite long in miniemulsion polymerization.[38,39]

It should be noticed that emulsion studies have tried to disperse dried O-MMT in aqueous or organic phase. In order to overcome aforementioned problems in synthesis of waterborne O-MMT–polymer nanocomposite via emulsion polymerization, a promising way is to mix O-MMT with monomers directly after the ion-exchange of Na-MMT with an organic modifier. As a result, O-MMT water dispersion is obtained soon after the organic modification. This method is the easiest way to obtain O-MMT water dispersion to be used in waterborne emulsion polymerization since dried O-MMT platelets cannot disperse in water due to its high hydrophobic surface. If a good MMT water dispersion, which leads to destruction of O-MMT platelets, is achieved in waterborne emulsion polymerization, polymerization can take place within the MMT platelets. By this method, drying process of O-MMT and effort for dispersing dried O-MMT in water or monomer phase are not required. Kiernowski *et al.* followed this procedure but they could obtain PMMA–O-MMT nanocomposite with low solids content (<25%).[40]

The goal of this study is to synthesize poly(butyl acrylate-co-methyl methacrylate) (Poly(BA-co-MMA)) nanocomposites in the presence of Na-MMT and O-MMT with high solids and clay content. Both Na-MMT and O-MMT nanocomposites were synthesized via semibatch emulsion polymerization. In order to achieve exfoliated O-MMT nanocomposite, O-MMT was used directly after the modification of Na-MMT with dimethyl dioctadecyl ammonium chloride (DMDOAC), so miniemulsion process was not needed. Poly(BA-co-MMA) nanocomposites were obtained with 35 wt % solids and 3 wt % Na-MMT or O-MMT content. Synthesizing O-MMT-poly(BA-co-MMA) via emulsion polymerization with such a high solid and O-MMT content has not been reported before in open literature. Furthermore, a more challenging issue of this study is that even poly(BA-co-MMA) nanocomposites with 47 wt % solids and 3 wt % Na-MMT or O-MMT content were synthesized.

EXPERIMENTAL

Materials

Raw Na-MMT (bentonite) was obtained from Resadiye, Turkey with cation exchange capacity (CEC) of 72.6 meq/100 g. Raw Na-MMT was purified before using in PCN synthesis and CEC increased to 120 meq/100 g. CEC of the samples were determined according to ASTM C837-09 standard. Dimethyl dioctadecyl ammonium chloride (DMDOAC) was used for organo-modification of Na-MMT. Butyl acrylate (BA), methyl methacrylate (MMA), and methacrylic acid (MAA) were supplied from Merck and used without further purification. MAA was used at a low ratio to help the stabilization of the latex. 1-Dodecanethiol (C_{12}-SH, Merck) was used as a chain transfer agent. Other pure chemicals were supplied from Aldrich such as potassium persulfate (KPS) as an initiator, sodium carbonate as a buffer, and sodium lauryl sulfate (SLS) as a surfactant.

Purification of Na-MMT and Preparation of O-MMT

In order to separate Na-MMT from associated minerals (quartz, calcite, etc.), raw sample was crushed and sieved under 2 mm. Particles under2 mm were dispersed in water at 60°C for 30 min. Then, the suspension was centrifuged at 5000 rpm for 20 min to remove undispersed particles (iron oxide, Ca-MMT, illite, etc.). As a result, raw Na-MMT was purified by this wet process. Four different Na-MMT suspensions with Na-MMT contents of 1.1, 1.6, 2.2, and 3.3 wt % were prepared in this way. These suspensions were directly used in PCN synthesis to set the Na-MMT ratios in copolymer and nanoadditive mixture as 1, 1.5, 2, and 3 wt % based on the total amount of monomers.

Organophilic MMT was prepared as follows: purified colloidal Na-MMT suspension (2.2 wt % of Na-MMT) was stirred for 30 min at 60°C. A water solution of DMDOAC (10 wt % of

Table I. Typical Recipe for Synthesis of Nanocomposites with 47 wt % Solids Content

Ingredients (g)	First stage	Second stage
Na-MMT suspension/O-MMT suspension/water	165	
SLS	0.65	
Sodium carbonate	0.45	
KPS	0.45	0.45
Monomer pre-emulsion	9	325.95
Na-MMT suspension/water	*72*	
SLS	*2.65*	
BA	*126*	
MMA	*126*	
MAA	*3.8*	
1-dodecenethiol	*4.5*	

DMDOAC), at a concentration equivalent to 1.8 times CEC of the Na-MMT, was slowly added to the suspension. After stirring for 30 min at 60°C, an O-MMT-water suspension with 1 wt % O-MMT was obtained. By controlled filtering of pre-prepared O-MMT suspension, four O-MMT suspensions having O-MMT contents of 1.1, 1.6, 2.5, and 3.3 wt % were obtained. These four suspensions were directly used in PCN synthesis to set the O-MMT ratios in copolymer and nanoadditive mixture as 1, 1.5, 2, and 3 wt % based on the total amount of monomers.

Synthesis of MMT-Acrylate Nanocomposites

Poly(BA-co-MMA)/Na-MMT waterborne nanocomposites were synthesized by seeded semibatch emulsion polymerization. Purified Na-MMT suspensions were used for nanocomposite synthesis. All reactions were carried out in a 1 L stirred tank glass reactor equipped with a jacket, reflux condenser, nitrogen inlet, two feeding inlets, and an anchor stirrer rotating at 200 rpm. A typical recipe for 47 wt % solid content is shown in Table I. In the first stage, seed was prepared by batch emulsion polymerization. Na-MMT suspension (165.0 g), SLS (0.65 g), and sodium carbonate (0.45 g) were added in the glass reactor and stirred while the mixture was heated to 80°C. Na-MMT suspension, before being added into the reactor, was sonified using Hielscher UP 400Sat 80% duty cycle for 10 min. After the reactor temperature stabilized at 80°C, KPS solution (0.45 g in 4 g of water) as an initiator was added into the reactor followed by the addition of 9 g monomer pre-emulsion. The mixture was stirred for 30 min at 80°C. Monomer pre-emulsion had been prepared by adding sonified Na-MMT suspension (72.0 g), SLS (2.65 g), BA (126 g), MMA (126 g), MAA (3.8 g), and $C_{12}SH$ (4.5 g) into a flask. The mixture had been stirred vigorously.

In the second stage of polymerization, the remaining monomer pre-emulsion was fed into the seed dispersion together with an initiator KPS aqueous solution (0.45 g in 4 g of water) with a total feeding time of 3 h. After the completion of addition, the system was allowed to polymerize 30 more minutes at 80°C. As a result, a dispersion with 47 wt % solids content was produced. Na-MMT suspensions with varying Na-MMT ratios, which were prepared as described in the previous section, were used for synthesizing nanocomposites having different Na-MMT contents.

O-MMT copolymer nanocomposites of varying O-MMT contents (47 wt % solids content) were prepared with the same method except using O-MMT suspension instead of Na-MMT suspension. O-MMT suspensions with varying O-MMT contents were prepared as described in the previous section. O-MMT suspensions were sonified before being added to the seed and pre-emulsion stages. Sonication played a critical role in synthesizing nanocomposites with high solids and low coagulum contents. By means of sonication, spaces between MMT platelets expanded and stabile MMT suspensions were formed.

To obtain Na-MMT and O-MMT polymer nanocomposites with 35 wt % solids and 3 wt % clay contents, 310 g Na-MMT/O-MMT and 150 g Na-MMT/O-MMT suspensions with 1.6 wt % Na-MMT/O-MMT were used in the seed stage and the pre-emulsion stage, respectively.

For comparison, pristine waterborne latex was synthesized following the same procedure except by using water instead of Na-MMT suspension. Final latex had 49 wt % solids content.

Moreover, physical blend of both sonified Na-MMT suspension and O-MMT suspension with pristine latex were examined for comparison sake. Table II shows a clear summary of all the experiments carried out.

Analyses and Characterizations

All nanocomposite films to be analyzed were prepared by pouring 15–20 mL nanocomposite dispersion on poly propylene circular surface with a diameter of 10 cm. Then, the nanocomposite dispersions were dried at 40°C till the constant

Table II. Summary of the Procedure for Synthesis of the Nanocomposites

Sample	Solids content (wt %)	Process	wt % MMT [a]	Type of MMT
L0	49	Emulsion-SemiBatch	-	-
MN1	47	Emulsion-SemiBatch	1	Na-MMT
MN2	47	Emulsion-SemiBatch	1.5	Na-MMT
MN3	47	Emulsion-SemiBatch	2	Na-MMT
MN4	47	Emulsion-SemiBatch	3	Na-MMT
MN5	35	Emulsion-SemiBatch	3	Na-MMT
MN6	35	Blend[b]	3	Na-MMT
OMN1	47	Emulsion-SemiBatch	1	O-MMT
OMN2	47	Emulsion-SemiBatch	1.5	O-MMT
OMN3	47	Emulsion-SemiBatch	2	O-MMT
OMN4	47	Emulsion-SemiBatch	3	O-MMT
OMN5	35	Emulsion-SemiBatch	3	O-MMT
OMN6	35	Blend[b]	1.5	O-MMT

[a] Based on the total amount of monomer.
[b] The polymer Na-MMT and O-MMT nanocomposites were prepared by blending MN1 with sonified Na-MMT or O-MMT suspension by stirring 500 rpm at 60°C for 1 h.

weight. Finally polymer films having 40–50 μm thickness were formed.

FTIR spectra of Na-MMT, O-MMT, and the nanocomposite films were taken on a Perkin Elmer Spectrum One FTIR Spectrometer. The recorded wavenumber was from 4000 to 400 cm^{-1}.

MMT samples and the nanocomposite films were analyzed by X-ray diffraction (XRD) using a SHIMADZU XRD-6000 model XRD instrument (Cu Ka radiation with $\lambda = 0.154$ nm). The range of the diffraction angle is $2\theta = 2$–40° with a scanning rate of 0.02°/s. The distances between MMT layers were calculated with Bragg's law: 2d sin $\theta = n\lambda$; where λ was the wavelength of the X-ray, d is the interspacing distance, and θ is the angle of incident radiation.

The particle size distributions of the nanocomposite emulsions were measured by light scattering using a Malvern Zetasizer Nano ZSP. Dried coagulum contents were determined in terms of the theoretical total mass of each synthesis by filtering the nanocomposite dispersions through an ASTM #200 sieve and then drying the sieve. Synthesis experiments were repeated three times for particle size distribution analysis and coagulum contents determination. Five measurements were made for each sample in particle size distribution analysis.

The gel contents of the samples were measured after the sieving process via conventional Soxhlet extraction, using tetrahydrofuran (THF) as solvent. A glass fiber disk was impregnated with a few drops of latex and the extraction was carried out for 24 h under reflux conditions at about 80°C. The gel remained in the glass fiber, whereas the polymer soluble fraction was recovered from THF solution. The amount of gel was calculated using the following equation:

$$\text{gel}(\%) = \frac{w_{\text{gel}} - (w_{\text{total}} \cdot x_{\text{clay}})}{w_{\text{total}} - (w_{\text{total}} \cdot x_{\text{clay}})} \times 100$$

where w_{gel} is the amount of insoluble polymer that remained in the glass fiber, w_{total} is the whole polymer sample, and x_{clay} is the fraction of clay content based on monomer in the formulation.

The glass transition temperature (Tg) of the nanocomposite films were determined by differential scanning calorimetry (DSC) using a Perkin Elmer Jade DSC instrument at a heating rate of 10°C/min under N_2 atmosphere from −40 to 200°C. All data were collected from a second heating cycle and the glass transition temperatures (Tg) were calculated as a midpoint of thermogram.

The final compositions of the nanocomposite films were determined by proton NMR in CDCl3 using a Bruker 500 MHz NMR spectrometer. The molecular weight distribution and the average molecular weights of the soluble polymer fraction were determined by gel permeation chromatography using an Agilent 1100 series.

The thermal stability of the nanocomposite films was studied by thermogravimetric analysis (TGA): heating in nitrogen atmosphere from 20 to 900°C with a heating rate of 10°C/min using Perkin Elmer Pyris1 TGA instrument.

The mechanical properties of the nanocomposite films were analyzed by testing machine Zwick Z250. The measurements were carried out applying a stretch force at 500 mm/min to the nanocomposite film. Five experiments were performed for each sample.

The barrier properties were investigated by measuring water vapor permeation and oxygen permeation of the nanocomposite films. Water vapor permeation test was carried out according to ASTM E 96-05. Oxygen permeability tests were carried out by using Labthink PERME-VAC-V2 instrument.

The morphology of the nanocomposites was studied by means of a transmission electron microscope, TEM (Jeol Jem 2100 HRTEM, acceleration voltage 200 kV).

Gloss measurements of the nanocomposite films were performed according to ASTM 523 by using Sheen Ltd gloss equipment. Gloss change was determined by the reflection angles of 20°, 60°, and 85°. Five measurements were made for each sample.

RESULTS AND DISCUSSION

Characterization of representative nanocomposites (MN1, MN3, and OMN3) along with those of Na-MMT and O-MMT was realized by evaluation of IR spectra (Figure 1). Transmittance peaks of Na-MMT show —OH stretching of silicate layers at 3450–3650 cm^{-1} and bending of the —OH groups at 1641 cm^{-1}, while Si—O stretching was observed at 1045 cm^{-1}. Si—O—Al bending vibrations were found in the range of 400–920 cm^{-1}. Peaks of O-MMT at 2850–2920 cm^{-1} represent the stretching vibrations of an alkyl group (CH_3). NH bending was found at 1469 cm^{-1}. Peaks observed at 2957 and 2875 cm^{-1} for MN1 (pristine poly BA-co-MMA latex) represent the aliphatic C—H stretching, while the peak at 1734 cm^{-1} represents C=O stretching. Further peaks at 1000–1250 cm^{-1} are attributed to C—O stretching. The characteristic peak at 752 cm^{-1} is assigned to the aromatic C—H bending due to poly(BA-co-MMA).

Characteristic Na-MMT and O-MMT peaks are not present in the spectra of the nanocomposites probably due to its low content and a possible overlapping on the absorption band of BA-co-MMA copolymer. On the other hand, an increase could also

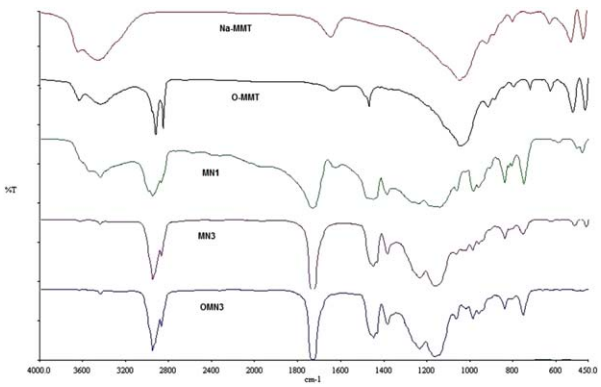

Figure 1. IR spectra of O-MMT, Na-MMT, and the nanocomposites. [Color figure can be viewed in the online issue, which is available at wileyonlinelibrary.com.]

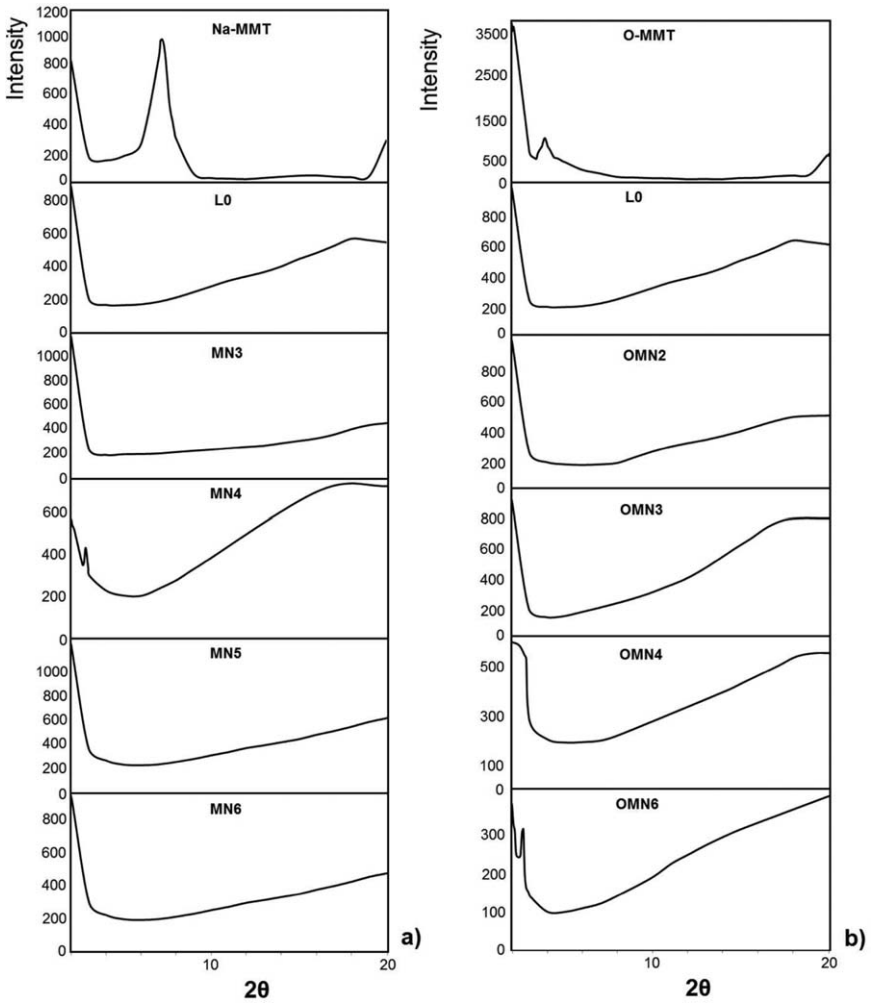

Figure 2. XRD patterns of some selected nanocomposite films and corresponding MMT: a) comparison of Na-MMT, O-MMT, latex without nanoadditive, and copolymer nanocomposites; b) comparison of O-MMT, latex without nanoadditive, and copolymer nanocomposites.

be observed at the peak intensity of the band 1068 cm^{-1}, which seems to suggest Si—O—Si absorption, and at the peak intensity of the band 1450 cm^{-1}, which is NH bending. In addition, the characteristic peak of C—C of BA-co-MMA copolymer at the stretching band of 1645 $cm^{-1}$was not observed in spectra of the nanocomposites.

The XRD patterns of Na-MMT, O-MMT, pristine BA-co-MMA copolymer (L0), and the BA-co-MMA copolymer-MMT nanocomposites (MN3, MN4, MN5, MN6, OMN2, OMN3, OMN4, and OMN6) appear in Figure 2. Na-MMT showed an interlayer spacing of $d = 1.15$ nm at 2θ value of 7.8° [Figure 2(a)]. In the patterns of MN3, MN5, and MN6 nanocomposites, the first peak corresponding to Na-MMT seems to be diminished, which suggests exfoliation of Na-MMT. Although Diaconu *et al.*[34–36] claimed that the nanocomposite obtained by physical blend showed tactoids and aggregates of MMT platelets, in this study, even the blend nanocomposite MN6 showed exfoliated structure according to the XRD pattern. This is possibly due to the sonication of Na-MMT suspension before blending process and mixing the copolymer and sonified Na-MMT at 60°C for 1 h during the blending process. MN4 nanocomposite which had 47 wt % solids and 3 wt % Na-MMT content showed a peak at $2\theta = 2.7°$ ($d(001) = 3.32$ nm). This peak is possibly a result of intercalated structure rather than exfoliation. However, characteristic clay peak was shifted to lower angle indicating good intercalation (with larger d-spacing) and possible evidence of few exfoliated structure.[41] Nevertheless, XRD results of MN4, MN3 (which had 47 wt % solids and 2 wt % Na-MMT content), and MN5 (which had 35 wt % solids and 3 wt % Na-MMT content) conclude that high solids and MMT content resulted in poor MMT dispersion within the copolymer matrix.

The prominent peak of O-MMT at 2.10° shows that the basal space of the pristine clay increased from 1.15 to 3.89 nm due to the presence of DMDOAC [Figure 2(b)]. OMN2, OMN3, and OMN4 nanocomposites, which were synthesized by semibatch emulsion polymerization, showed no peak in the XRD pattern indicating that O-MMT particles were dispersed homogenously and exfoliated in the copolymer matrix. However, OMN6 nanocomposite (blend) exhibited a peak at 2.6° ($d(001) = 3.39$ nm), revealing that exfoliated structure could not be achieved for OMN6 nanocomposite. In "in situ polymerization," polymerization taking place between MMT platelets increased interlayer

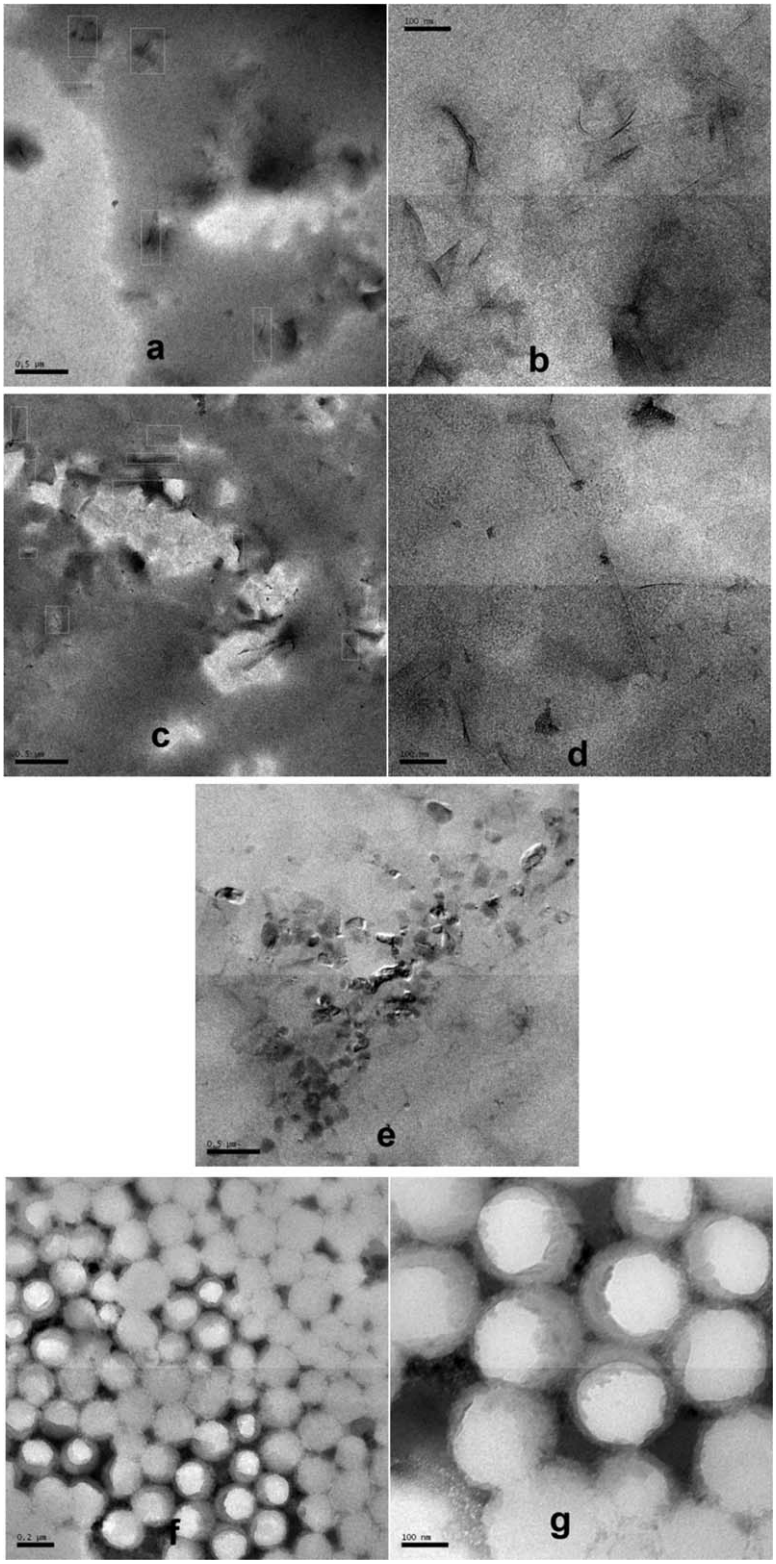

Figure 3. TEM images of nanocomposites: (a,b) MN3; (c,d) MN6; (e) MN4; and (f,g) OMN2.

spacing and exfoliation of MMT platelets. However, in blending process hydrophobic O-MMT could not disperse in polymer–water mixture sufficiently. That is why, in contrast to Na-MMT, O-MMT blend could not permit exfoliation.

In addition to XRD analyses, nanocomposites were also analyzed by TEM to investigate the structure of MMT in the polymer matrix. TEM micrographs of the some representative nanocomposites at different magnifications are shown in Figure

Table III. Properties of Nanocomposites

Sample	Average particle size (nm)	Gel fraction (%)	Coagulum (%)	Mn ($\times 10^3$)	Mw ($\times 10^3$)	Mwd	*Tg* (°C)
L0	117.6 ± 2.1	0.1	0.12 ± 0.02	1.69	3.27	1.93	9.2 ± 0.2
MN1	119.1 ± 1.8	0.2	0.15 ± 0.02	1.71	3.30	1.93	9.2 ± 0.2
MN2	118.4 ± 1.2	0.1	0.14 ± 0.04	1.66	3.18	1.92	9.4 ± 0.1
MN3	117.5 ± 0.9	0.2	0.30 ± 0.04	1.74	3.13	1.80	12.5 ± 0.6
MN4	152.4 ± 3.4	0.2	3.11 ± 0.12	1.73	3.11	1.80	9.3 ± 0.3
MN5	117.2 ± 2.3	0.1	0.17 ± 0.04	1.64	3.41	2.08	9.2 ± 0.2
MN6	127.4 ± 1.5	0.2	0.15 ± 0.05	1.79	3.68	1.97	12.1 ± 0.4
OMN1	209.5 ± 1.9	0.1	0.22 ± 0.04	1.58	3.12	1.97	9.1 ± 0.2
OMN2	200.7 ± 2.3	0.1	0.34 ± 0.03	1.64	3.21	1.96	10.3 ± 0.3
OMN3	292.9 ± 3.2	0.2	0.81 ± 0.04	1.72	3.14	1.83	12.3 ± 0.3
OMN4	335.1 ± 3.3	0.2	4.08 ± 0.22	1.71	3.09	1.81	10.4 ± 0.2
OMN5	264.8 ± 1.8	0.1	0.77 ± 0.06	1.59	3.21	2.02	11.9 ± 0.1
OMN6	120.0 ± 2.4	0.1	1.54 ± 0.07	1.65	3.12	1.89	9.9 ± 0.1

3. The micrographs show that exfoliated and intercalated structures were obtained in the nanocomposites containing Na-MMT (MN3 and MN6). A large number of individual MMT platelets can be clearly distinguished. For nanocomposite MN4, the structure is different. MMT was not well dispersed in the medium and the aggregates of MMT platelets could be seen. Thus, TEM micrographs are lending support to the determinations based on XRD pattern analyses. Unfortunately, the O-MMT platelets could not be clearly distinguished in the images of nanocomposite OMN2. Similar situations have been reported in previous studies.[42–44] According to Micusik *et al.*,[44] spherical particles in TEM images are the sign that MMT is not located at the surfactant. Based on TEM images, it seems that the use of more surface agents caused the formation of circle nanoparticles, with the increasing of size, depending on the concentration of O-MMT.

The average particle size, molecular weight (Mn and Mw), molecular weight distribution (Mwd), gel fraction, coagulum, and Tg of the nanocomposites are given in Table III. Average particle size of the pristine copolymer was 117.6 nm. Particle size did not change with Na-MMT addition to the medium. Only MN4 nanocomposite had greater size (152.4 nm), revealing that increasing concentration of Na-MMT and solids content probably caused aggregation as described by Diaconu *et al.*[34]

On the other hand, substantial increase in the particle size was observed when adding O-MMT to the medium. Average particle size of OMN1, which had 1 wt % O-MMT, was 209.5 nm and average particle size increased with increasing concentration of O-MMT particles. Increase in the average particle size could be caused by surfactants enabling the entry of monomers into the MMT platelets. Therefore, more surfactant entered into the MMT platelets when MMT content increased and the amount of surfactant in the medium decreased. This situation caused a decrease in the number of particles and an increase in particle size.[45,46] However, this effect was not observed in Na-MMT nanocomposites probably because of the lower *d*-space of Na-MMT platelets and weak affinity between the Na-MMT and the copolymer. OMN5 (with low solids content) nanocomposite having lower mean particle size than OMN4 also confirms that the particle size of nanocomposite got higher with increasing concentration of solids. The mean particle size of OMN6 (blend) nanocomposite was close to that of blank polymer MN1, showing that physical blending had no effect on particle size.

Gel fractions of all samples were similar and around 0.1–0.2%. Addition of nanoparticles had no effect on gel formation.

Synthesized nanocomposites were coagulum-free except MN4, OMN3, and OMN4. Coagulum in nanocomposite samples indicates unreacted monomers as well as undispersed MMT. MN4 nanocomposite had coagulum of 3.11%. This is an expected situation since an MMT suspension containing 3 wt % Na-MMT is even viscous. In this study, O-MMT copolymer nanocomposites were synthesized directly after the ion-exchange of organic cation with a suspension of the Na-MMT, so a water dispersion of O-MMT was used in nanocomposite synthesis. Due to the fact that O-MMT's dispersion in water is poor contrary to Na-MMT, at higher solids and O-MMT contents (OMN3 and OMN4), agglomerations (coagulum) of O-MMT nanocomposites were slightly higher than that of Na-MMT nanocomposites. However, coagulum of OMN3 was low and at negligible levels since O-MMT content in OMN3 was not as high as in OMN4.

Molecular weight of poly(BA-co-MMA) is directly related to the amount of chain transfer agent and indirectly related with the ratio of BA and MMA in polymer. According to proton NMR, final composition of the blank copolymer MN1 and nanocomposites were quite close to each other (MMA: 0.55–0.57; BA: 0.43–0.45). Proton NMRs of some representative samples are given in Figure 4. Molecular weights of the copolymers were tried to be kept constant about 17,000 by keeping MMA: BA

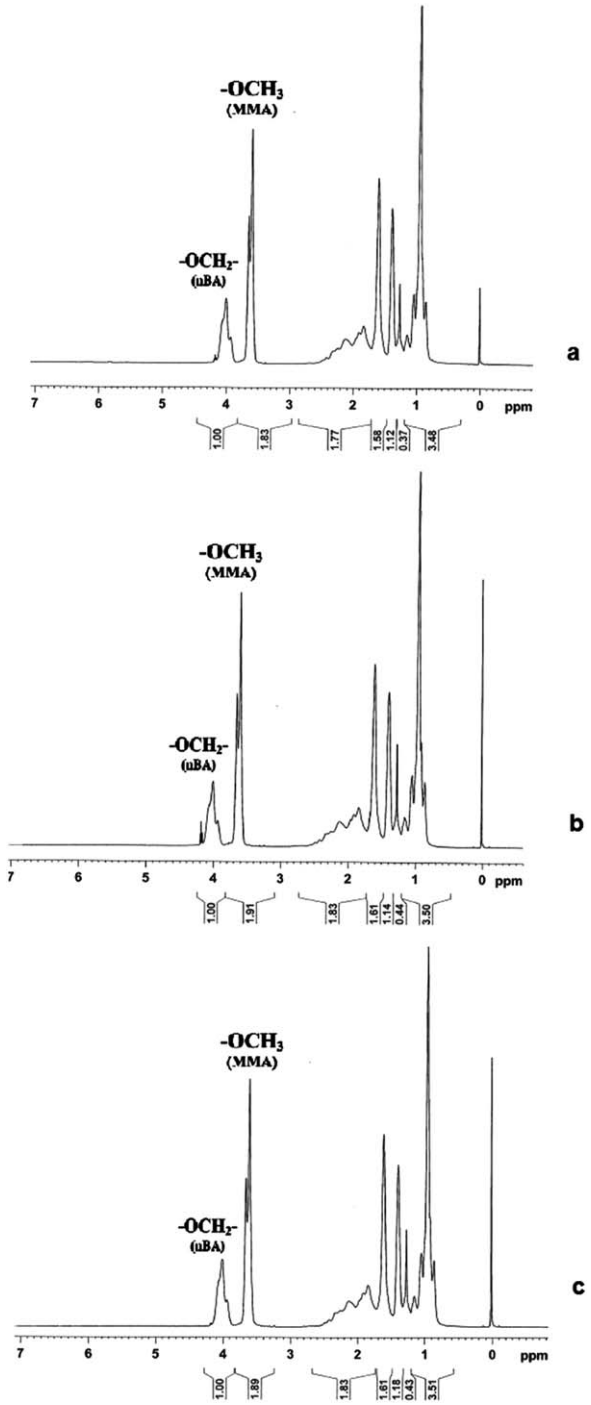

Figure 4. ^{1}H NMR spectra of (a) MN1, (b) MN4, and (c) OMN4.

ratio and the amount of the chain transfer agents constant. Molecular weights, Mn and Mw, of the all copolymers were close to each other and molecular weight distribution Mwd was approximately between 1.8 and 2.

Presence of Na-MMT and O-MMT increased Tg of polymer slightly, but it is not possible to observe Tg change as a function of MMT content. Perhaps this situation is related to the low level of exfoliation of MMT platelets in some nanocomposites.[47] Closer Tg values also make comparison difficult due to measurement errors. Nevertheless, MN3, MN6, OMN3, and OMN5 had higher Tg values of 12.5 ± 0.6, 12.1 ± 0.4, 12.3 ± 0.3, and 11.9 ± 0.1°C, respectively. These Tg values confirm that good MMT dispersion at high MMT contents could increase Tg values of polymers more explicitly. Furthermore, higher Tg values could be the sign of better exfoliation for those nanocomposites. However, it could be stated that Tg increment was not so high (about °C) compared to pristine copolymer (9.2°C). In other words, the presence of MMT did not have strong effect on the retardation of molecular mobility of polymers.

Table IV. Thermal Stabilities of the Samples

	T_d (°C)		
Sample	10 wt % loss	50 wt % loss	Remaining mass wt %
L0	369.7	398.6	0.54
MN1	381.9	418.4	1.84
MN2	381.4	418.9	2.10
MN3	384.1	421.0	2.65
MN4	384.9	420.1	2.95
MN5	386.2	421.7	3.22
MN6	387.7	422.5	3.34
OMN1	374.4	409.3	1.27
OMN2	385.8	412.8	1.18
OMN3	387.3	414.1	0.85
OMN4	377.3	411.3	0.99
OMN5	382.9	414.5	0.81
OMN6	371.1	411.6	0.97

Thermal degradation of the nanocomposites was investigated by TGA. Residual mass of the samples at 900°C and decomposition temperatures (Td) of the samples at 10 and 50 wt % weight losses are listed in Table IV. Higher residual mass remaining in the nanocomposites when compared to the pure polymer indicates the presence of MMT in the medium. The Td of nanocomposite films at 10 and 50 wt % weight loss increased significantly compared to pristine polymer. According to Vyazovkin *et al.*, during nanocomposite degradation, MMT platelets move gradually to the surface of nanocomposite due to a decrease in the surface free energy. Accordingly, MMT provides thermal barrier to the nanocomposite.[48] The shift in Td could be clearly seen from TGA curves and the derivative curves of TGA thermograms (Figure 5). Increase of the content of both Na-MMT and O-MMT caused improvement in thermal stability by shifting the decomposition temperature to higher values. However, Td of MN4, OMN4, and OMN6 did not follow the trend probably due to the low exfoliation of MMT platelets. Na-MMT ensured higher increase than O-MMT in the decomposition temperature. Td of Na-MMT-based nanocomposites were between 418.4 and 422.5°C at 50 wt % weight loss while Td of O-MMT-based nanocomposites were between 409.3 and 414.5°C. It is probably because of the decomposition of organic cation in O-MMT at 270–330°C, which caused the remaining MMT mass in O-MMT nanocomposites becoming less than that of Na-MMT nanocomposites. Thus, the decomposition

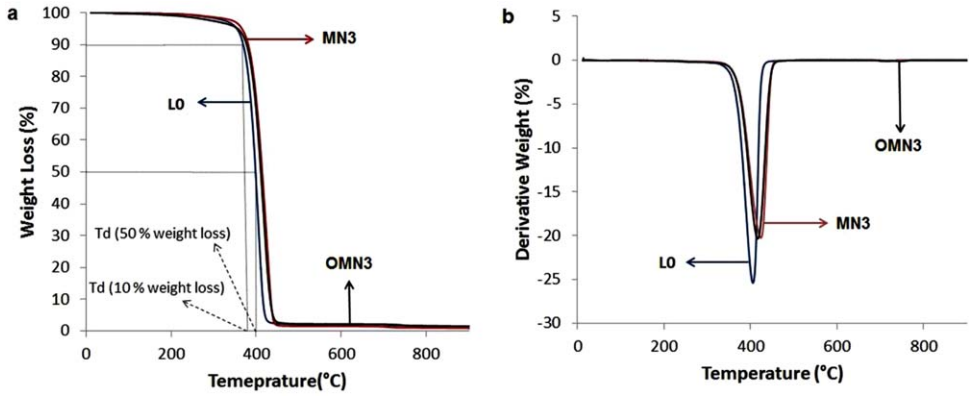

Figure 5. Representative (a) TGA curves and (b) Derivative curves of TGA thermograms. [Color figure can be viewed in the online issue, which is available at wileyonlinelibrary.com.]

temperature increments of O-MMT nanocomposites were lower than Na-MMT nanocomposites. Along with these consequences, Td of MN5, MN6, OMN5, and OMN6 nanocomposites suggests that process type (emulsion or blend) and solids content had no certain effect on thermal stability.

Mechanical properties of the samples are shown in Figure 6. The three main parameters of mechanical measurements are (i) tensile strength, which is the stress needed to break a sample, (ii) elastic modulus, which is a measure of elastic response to the deformation, and (iii) elongation at break, which is the strain on a sample when it breaks.[49] The interactions at the interface between the copolymer matrix and MMT platelets decreased mobility in the copolymer particles near the interface, which improved mechanical properties.[50] Average tensile strength of pristine copolymer L0 was 4.0 MPa. Na-MMT nanocomposites MN1, MN2, MN3, MN5, and MN6 had average tensile strength of 4.5, 5.0, 6.2, 7.5 and 7.5 MPa, respectively. Average tensile strengths of O-MMT nanocomposites OMN1, OMN2, OMN3, and OMN5 were 4.5, 5.0, 6.4, and 7.5 MPa, respectively. Tensile strength increased with an increase in both Na-MMT and O-MMT loading. This is in agreement with the literature results.[34–36,51,52] However, average tensile strengths of MN4 (5.8 MPa) and OMN4 (6.0 MPa) were lower than MN3 and OMN3, respectively, although MMT contents were higher

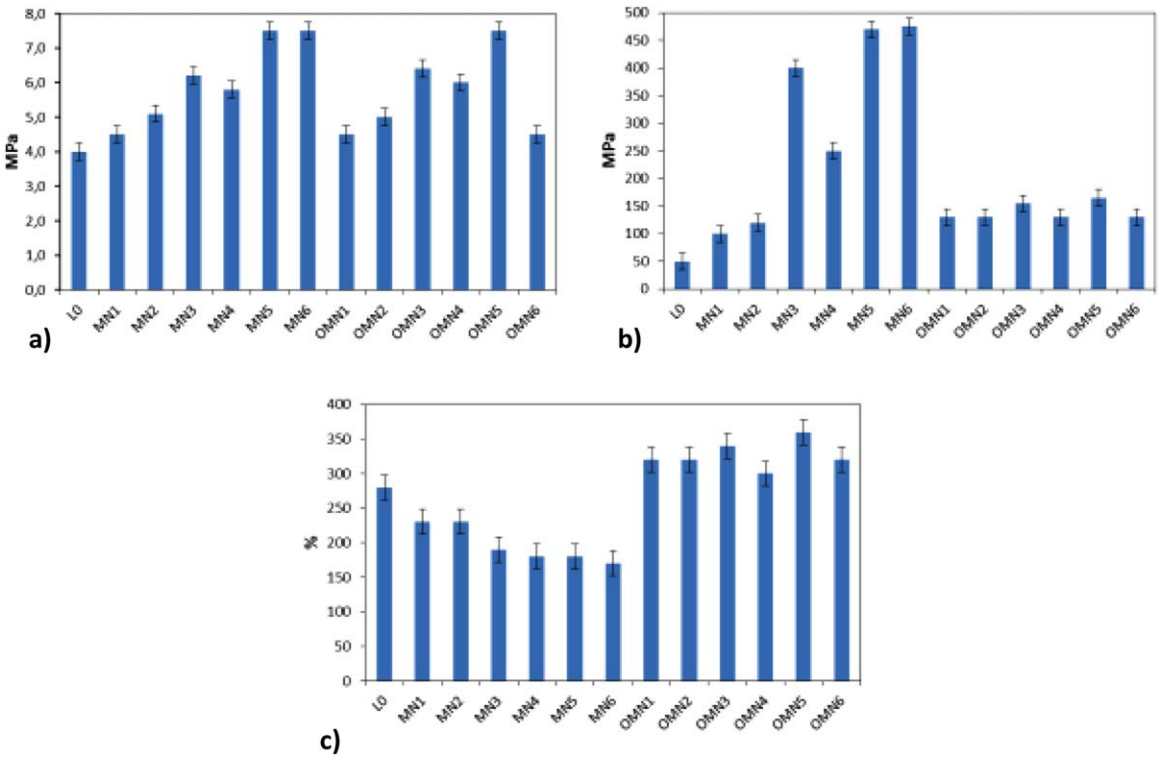

Figure 6. (a) Tensile strength, (b) elastic modulus, and (c) elongation at break values of the samples. [Color figure can be viewed in the online issue, which is available at wileyonlinelibrary.com.]

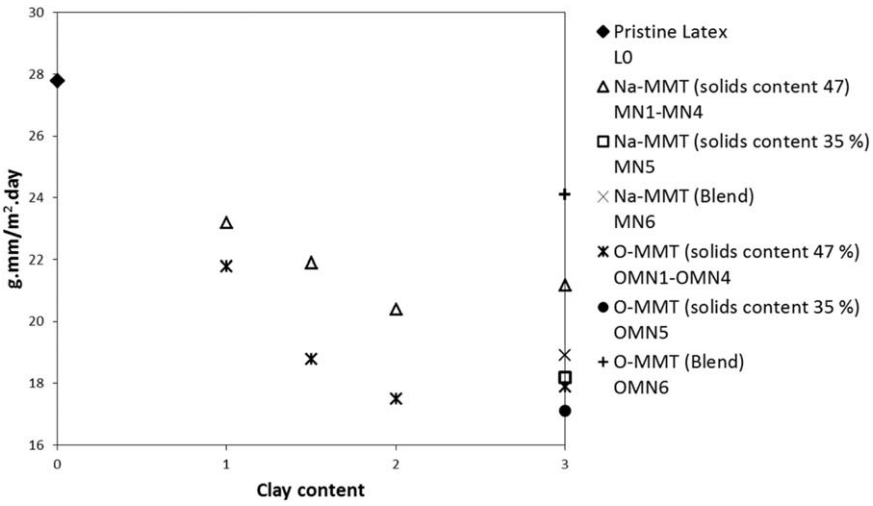

Figure 7. WVTR of the samples.

for MN4 and OMN4. It is generally known that exfoliation of MMT platelets in polymer matrix is an important factor to enhance mechanical properties of the polymer. Tensile strength of MN4 and OMN4 were lower since they had intercalated structure rather than exfoliated due to the high solids content of the dispersion. High solids content made the medium viscous, so MMT platelets could not delaminate sufficiently. Tensile strength of OMN6 (4.5 MPa), which was prepared by blending process, was lower than the other nanocomposites since blending process did not ensure sufficient O-MMT dispersion in polymer matrix. Tensile strengths of Na-MMT and O-MMT nanocomposites, which had same Na-MMT and O-MMT contents, were similar. Thus, there was no clear difference between O-MMT and Na-MMT nanocomposites in terms of tensile strength. However, elongation at break for Na-MMT nanocomposites decreased, while slight increases were observed in O-MMT nanocomposites' elongations. A similar behavior has been reported for other polymer nanocomposites in a number of studies.[52–54] This kind of behavior is probably due to the fact that organic modification of MMT could increase the enhancement in the interfacial interaction between MMT and the copolymer.[55]

Elastic modulus is the ratio of tensile stress along an axis to the strain. Consequently, elastic modulus values of nanocomposites were higher than that of pure copolymer and Na-MMT was more effective than O-MMT. Elastic modulus could increase to 475 ± 30 MPa for Na-MMT nanocomposites (MN6), while O-MMT nanocomposites showed maximum 165 ± 20 MPa elastic modulus (OMN5).

Table V. Gloss Values of the samples at 20°, 60°, and 85°

	Gloss Measurement		
Sample	20°	60°	85°
MN1	110 ± 3	140 ± 6	75 ± 2
MN2	88 ± 4	112 ± 2	71 ± 2
MN3	58 ± 3	85 ± 2	62 ± 1
MN5	39 ± 4	71 ± 3	50 ± 3
OMN1	128 ± 6	155 ± 4	81 ± 2
OMN2	132 ± 4	163 ± 2	82 ± 2
OMN3	135 ± 5	170 ± 2	85 ± 4
OMN4	125 ± 2	155 ± 3	83 ± 3

Barrier properties were tested through water vapor transmission rates (WVTR), as shown in Figure 7. WVTR of L0 was 27.8 g mm/m^2 day. It can be noted that WVTR decreased for all the nanocomposites when compared to the pristine copolymer, due to tortuosity of the diffusion pathway of water through the films.[56] Further increase in Na-MMT and O-MMT loading improved barrier property. However, MN4, OMN4, and OMN6 did not follow the trend, as expected since these nanocomposites had poor dispersion of MMT platelets. WVTR decreased to minimum 18.2 g mm/m^2 day (MN5) for Na-MMT nanocomposites and 17.1 (OMN5) g mm/m^2 day for O-MMT nanocomposites. WVTR of Na-MMT nanocomposites are higher compared to O-MMT nanocomposites at same nanoadditive contents, showing that low interfacial adhesion in Na-MMT nanocomposites causes lower compatibility and deterioration of barrier properties. Oxygen permeability test was also conducted for pristine latex, MN5, and OMN5 to support WVTR results. Oxygen permeability of pristine latex was 549 mL/m^2 day, whereas oxygen permeability of Na-MMT nanocomposite MN5 and O-MMT nanocomposite OMN5 were 441 and 402 mL/m^2 day, respectively. Oxygen permeability test revealed that nanoadditive improved oxygen permeability and O-MMT was more effective than Na-MMT as in the water vapor permeability test.

Gloss is a reflection of light and represents the shininess of a coating. MMT nanoparticles have been found to decrease coating gloss in some studies. This decline is supposed to be due to the surface roughness created by MMT particles.[57,58] On the other hand, there are many studies in literature showing that MMT additives increased gloss of polymer films.[59–62] The gloss measurements of the nanocomposites are presented in Table V. Gloss values of O-MMT nanocomposites were higher than that of pure copolymer and further increased with loading of O-MMT up to 2 wt %. However, gloss value decreased with

increasing O-MMT content over 2 wt %. Increase in gloss value can be related to good cross-linking of copolymer and can be the sign of good exfoliation, resulting in a smooth surface.[61] Gloss values of Na-MMT nanocomposites declined significantly, confirming this phenomenon. Affinity between the copolymer and MMT was weak since there was not enough compatibility between hydrophilic Na-MMT and the copolymer. Therefore, surface of the nanocomposite became less slippery due to increased roughness.[53,55]

CONCLUSIONS

Poly(BA-co-MMA)-MMT waterborne nanocomposites were successfully synthesized by semibatch emulsion polymerization technique and blending process for comparison. In this study, various nanocomposites were obtained containing Na-MMT or O-MMT between 1 and 3 wt % contents.

- Synthesizing Na-MMT nanocomposite by emulsion polymerization is well known. However, in this study, O-MMT was directly used in emulsion polymerization immediately after the organic modification of Na-MMT.
- Stable nanocomposites with 35 wt % solids content and 3 wt % Na-MMT or O-MMT content were obtained without any coagulum. The synthesis of nanocomposite containing 47 wt % solids was also achieved, but slight coagulum (1–4%) formed at high MMT contents. As a result, the poly(BA-co-MMA)-MMT nanocomposite containing the highest solid and MMT content in the literature was synthesized.
- Average particle sizes of Na-MMT nanocomposites were measured as 110–150 nm while O-MMT nanocomposites were measured as 200–350 nm.
- Furthermore, waterborne nanocomposites were prepared by blending pure copolymer latex with Na-MMT or O-MMT. However, O-MMT blend showed weak properties relative to Na-MMT blend and the other O-MMT-based nanocomposites.
- All nanocomposite samples were characterized by using various methods. XRD and TEM results indicated that waterborne poly(BA-co-MMA)-MMT nanocomposites with intercalated or exfoliated structures were achieved except MN4 and OMN6. DSC results revealed that the addition of MMT particles increased glass transition temperature of the copolymer slightly. The decomposition temperatures of the nanocomposites clearly increased with the addition of MMT particle according to TGA results. In the mechanical testing studies, tensile strength and storage modulus of all nanocomposites were higher than the pure copolymer while elongation at break decreased slightly for the films containing Na-MMT. Mechanical tests showed that exfoliated morphologies enhanced mechanical properties exceptionally relative to the intercalated/aggregated morphologies. All of the nanocomposites exhibited improved barrier properties in terms of WVTR. Oxygen permeability test also revealed that Na-MMT and O-MMT additive decreased oxygen permeability. The gloss values of O-MMT nanocomposites were found to be higher than that of the pristine copolymer, whereas Na-MMT nanocomposites exhibited less brightness. Consequently, elongation at break, barrier and gloss results exhibited that compatibility between O-MMT and copolymer was higher when compared to Na-MMT. In addition it was observed that MN4, OMN4, and OMN6 which had low exfoliation degree, showed poor properties.

In conclusion, some of the nanocomposites synthesized in this study can be used as waterborne binders for coating applications.

This work is financially supported by The Scientific and Technological Research Council of Turkey (TUBITAK) through the National support program. The authors thank Nevin Bekir and Zekayi Korlu for their valuable technical assistance in laboratory and Filli Boya A. Ş. for gloss measurements. Operation of TEM was possible with the help of Özgür Duygulu.

REFERENCES

1. Kojima, Y.; Usuki, A.; Kawasumi, M.; Okada, A.; Kurauchi, T.; Kamigaito, O. *J. Polym. Sci., Part A-1: Polym. Chem.* **1993**, *31*, 983.
2. Giannelis, E. P. *Adv. Mater.* **1996**, *8*, 29.
3. Gilman, J. W.; Jackson, C. L.; Morgan, A. B.; Harris, R. H.; Manias, E.; Giannelis, E. P.; Wuthenow, M.; Hilton, D.; Phillips, S. H. *Chem. Mater.* **2000**, *12*, 1866.
4. Okada, A.; Usuki, A. *Macromol. Mater. Eng.* **2006**, *291*, 1449.
5. Nguyen, Q. T.; Baird, D. G. *Polymer* **2007**, *48*, 6923.
6. Alexandre, M.; Dubois, P. *Mater. Sci. Eng.* **2000**, *28*, 1.
7. Haraguchi, K.; Takada, T. *Macromol. Chem. Phys.* **2014**, *215*, 295.
8. Haraguchi, K.; Farnworth, R.; Ohbayashi, A.; Takehisa, T. *Macromolecules* **2003**, *36*, 5732.
9. Huang, X.; Brittain, W. J. *Macromolecules* **2001**, *34*, 3255.
10. Nobel, M. L.; Picken, S. J.; Mendes, E. *Prog. Org. Coat.* **2007**, *58*, 96.
11. Lee, D. C.; Jang, L. W. *J. Appl. Polym. Sci.* **1996**, *61*, 1117.
12. Noh, M. H.; Lee, D. C. *J. Appl. Polym. Sci.* **1999**, *74*, 2811.
13. Noh, M. H.; Jang, L. W.; Lee, D. C. *J. Appl. Polym. Sci.* **1999**, *74*, 179.
14. Noh, M. H.; Lee, D. C. *Polym. Bull.* **1999**, *42*, 619.
15. Jang, L. W.; Kang, C. M.; Lee, D. C. *J. Polym. Sci., Part B: Polym. Phys.* **2001**, *39*, 719.
16. Choi, Y. S.; Choi, M. H.; Wang, K. H.; Kim, S. O.; Kim, Y. K.; Chung, I. J. *Macromolecules* **2001**, *34*, 8978.
17. Choi, Y. S.; Wang, K. H.; Xu, M.; Chung, I. J. *Chem. Mater.* **2002**, *14*, 2936.
18. Kim, Y. K.; Choi, Y. S.; Wang, K. H.; Chung, I. J. *Chem. Mater.* **2002**, *14*, 4990.
19. Choi, Y. S.; Xu, M.; Chung, I. J. *Polymer* **2005**, *46*, 531.
20. Yeh, J. M.; Liou, S. J.; Lai, M. C.; Chang, Y. W.; Huang, C. Y.; Chen, C. P.; Jaw, J. H.; Tsai, T. Y.; Yu, Y. H. *J. Appl. Polym. Sci.* **2004**, *94*, 1936.
21. Li, H.; Yu, Y.; Yang, Y. *Eur. Polym. J.* **2005**, *41*, 2016.
22. Park, B. J.; Choi, H. J. *Solid State Phenom.* **2006**, *111*, 187.
23. Wang, T.; Wang, M.; Zhang, Z.; Ge, X.; Fang, Y. *Mater. Lett.* **2006**, *60*, 2544.
24. Meneghetti, P.; Qutubuddin, S. *Langmuir* **2004**, *20*, 3424.

25. Asua, J. M. *Prog. Polym. Sci.* **2002**, *27*, 1283.
26. Houillot, L.; Nicola, J.; Save, M.; Charleux, B. *Langmuir* **2005**, *21*, 6726.
27. Mouran, D.; Reimers, J.; Schork, F. J. *J. Polym. Sci., Part A-1: Polym. Chem.* **1996**, *34*, 1073.
28. Cauvin, S.; Colver, P. J.; Bon, S. A. F. *Macromolecules* **2005**, *38*, 7887.
29. Sun, Q.; Deng, Y.; Wang, Z. L. *Macromol. Mater. Eng.* **2004**, *289*, 288.
30. Moraes, R. P.; Valera, T. S.; Demarquette, N. R.; Oliveira, P. C.; Da Silva, M. L. C. P.; Santos, A. M. *J. Appl. Polym. Sci.* **2009**, *112*, 1949.
31. Khezri, K.; Asl, V. H.; Mamaqani, H. R.; Kalajahi, M. S. *J. Polym. Eng.* **2012**, *32*, 111.
32. Khezri, K.; Asl, V. H.; Mamaqani, H. R.; Kalajahi, M. S. *J. Polym. Res.* **2012**, *19*, 1.
33. Li, D.; Zhang, M.; Wang, G.; Xing, S. *New J. Chem.* **2014**, *38*, 2348.
34. Diaconu, G.; Asua, J. M.; Paulis, M.; Leiza, J. R. *Macromol. Symp.* **2007**, *259*, 305.
35. Diaconu, G.; Paulis, M.; Leiza, *Macromol. React. Eng.* **2008**, *2*, 80.
36. Diaconu, G.; Paulis, M.; Leiza, *Polymer* **2008**, *49*, 2444.
37. Chanda, M. Introduction to Polymer Science and Chemistry: A Problem-Solving Approach, 2nd ed.; CRC Press: USA, **2013**, Chapter 11, pp 592.
38. Chern, C. S. In Encyclopedia of Surface and Colloid Science: Polymerization of Monomer Emulsions, 2nd ed.; Somasundaran, P., Ed.; CRC Press: USA, **2006**, Vol. *6*, pp 4990.
39. Chern, C. S. Principles and Applications of Emulsion Polymerization; John Wiley & Sons: New Jersey, **2008**, Chapter 5, pp 145.
40. Kiersnowski, A.; M. Wlazlak, T.; Dolega, J.; Piglowski, J. *e-Polym.* **2006**, *6*, 912.
41. Yilmaz, O.; Cheaburu, C. N.; Durraccio, D.; Gulumser, G.; Vasile, C. *Appl. Clay Sci.* **2010**, *49*, 288.
42. Diaconu, G.; Micusik, M.; Bonnefond, A.; Paulis, M.; Leiza, J. R. *Macromolecules* **2009**, *42*, 3316.
43. Zhang, Z.; Zhao, N.; Wei, W.; Wu, D.; Sun, Y. *Studies in Stud. Surf. Sci. Catal.* **2005**, *156*, 529.
44. Micusik, M.; Bonnefond, A.; Paulis, M.; Leiza, J. R. *Eur. Polym. J.* **2012**, *48*, 896.
45. Mirzataheri, M.; Mahdavian, A. R.; Atai, M. *Colloid Polym. Sci.* **2009**, *287*, 725.
46. Mirzataheri, M.; Mahdavian, A. R.; Atai, *Polym. Int.* **2011**, *60*, 613.
47. Reyes, Y.; Peruzzo, P. J.; Fernandez, M.; Paulis, M.; Leiza, J. R. *Langmuir* **2013**, *29*, 9849.
48. Vyazovkin, S.; Dranca, I.; Advincula, R. *J Phys Chem B* **2004**, *108*, 11672.
49. Jang, B. Z. Advanced Polymer Composites: Principles and Applications; ASM International: Materials Park, OH, **1994**.
50. Samakande, A.; Sanderson, R. D.; Hartmann, P. C. *Polymer* **2009**, *50*, 42.
51. Sirapanichart, S.; Monvisade, P.; Siriphannon, P.; Nukeaw, J. *Iran. Polym. J.* **2011**, *20*, 803.
52. Ning, W.; Xingxiang, Z.; Na, H.; Shihe, B. *Carbohydr. Polym.* **2009**, *76*, 68.
53. Dean, K.; Yu, L.; Wu,D. Y. *Compos. Sci. Technol.* **2007**, *67*, 413.
54. Chivrac, F.; Pollet, E.; Schmutz, M.; Averous, L. *Biomacromolecules* **2008**, *9*, 896.
55. Zhang, J. P.; Wang, A. Q. *Express Polym. Lett.* **2009**, *3*, 302.
56. Okamoto, M. *Encycl. Nanosci. Nanotechnol.* **2004**, *8*, 791.
57. Inceoglu, F.; Dalgicdir, C.; Menceloglu, Y. Z. Effect of Organoclay on the Physical Properties of UV-Curable Coatings, ACS Symposium Series 1008; American Chemical Society: Washington, DC, **2009**; p 270.
58. Tarablsi, B.; Delaite, C.; Brendle, J.; Barghorn, C. C. *Nanomaterials* **2012**, *2*, 413.
59. Doah, J. G. (Rohm and Haas Co.). World Patent WO03033559, April 3, 2003.
60. Zafar, F.; Zafar, H.; Sharmin, E. *J. Appl. Polym. Sci.* **2014**, *131*, 1.
61. Das, G.; Karak, N. *Polym. Degrad. Stab.* **2009**, *94*, 1948.
62. Garea, S. A.; Iovu, H. *Prog. Org. Coat.* **2006**, *56*, 319.